A COMPLETE OTA FREQUENCY MODEL

Eduard Alarcón, Alberto Poveda and Eva Vidal

Department of Electronic Engineering.
Polytechnic University of Catalonia. 08034 Barcelona. Spain.
Contact Address: ealarcon@eel.upc.es

IEEE 39th Midwest Symposium on Circuits and Systems (MWSCAS96)
Vol.1, pp 455-458, Ames, Iowa State University, August 18-21, 1996

A COMPLETE OTA FREQUENCY MODEL

EDUARD ALARCÓN , ALBERTO POVEDA AND EVA VIDAL
DEPARTMENT OF ELECTRONIC ENGINEERING. UNIVERSITY POLYTECHNIC OF CATALONIA. 08034 BARCELONA. SPAIN.
CONTACT ADDRESS: EALARCON@PETRUS.UPC.ES

Abstract. *A complete model for the Operational Transconductance Amplifier (OTA) is presented. The model includes the transconductance frequency response, the input bias current to output current transfer function, as well as the dependence of both input and output impedances on input bias current. This model is suitable for being included in complex simulation macromodels or used in analytical calculations. Simulation results and comparisons are also presented.*

1 . INTRODUCTION

The high operation speed in current-mode circuits and current-mode signal processing has generated some interest in relatively recent works. As long as the OTA converts the voltage signal into a current signal, it becomes an important current-mode building block. In addition to this, OTAs are, by themselves, of interest when designing electronically tunable analog filters and oscillators since their transconductance is linearly adjustable or programmable via an external current signal.

However, neither the manufacturer's specifications nor other papers provide a complete characterization of the OTA's frequency response and its dependence with DC bias current, I_{BIAS}. Therefore, a thorough description of OTA's frequency response is required so as to extend the frequency margin of possible designs. The need arises to have an accurate model of transfer functions (from differential voltage input and from bias dynamic current to output) and impedances with their dependencies on frequency and bias DC current.

Section 2 presents an overview of the key behavioral features of the OTA. This section provides the derivation of the OTA's frequency response. In section 3, a macromodel is obtained from the inclusion of previous section results in a Boyle-style macromodel. This macromodel includes several effects such as temperature dependence, input non-linearity and output clipping, as well as the proposed new features such as frequency dependent transconductance, transfer function between control and input, and impedance dependence on bias. Simulation results are also presented in section 3.

2. OTA BEHAVIOR FOR MODELING PURPOSES

The ideal small-signal OTA model shows its performance as a voltage controlled current source (VCCS). However, second order parasitic effects must be taken into account in the model, since they affect the performance of circuits using OTAs. Previous conceptual models [1] include finite input and output impedances, frequency-dependent transconductance gain (one pole) and input voltage nonlinearity, resulting in output current saturation. Nevertheless, not all the characteristics of the real device are modeled properly. Hence, an analysis of the different stages is required. Fig.1 depicts the internal block structure of a bipolar OTA (LM13600).

OTA's input and output impedances can be derived from small-signal parameters of bipolar transistors [2]. Taking into account figure 1, and assuming collector bias current of each transistor to be half of the external control current ($I_C = I_{bias}/2$), the input resistance can be expressed as:

$$R_{in} = \frac{V_{id}}{i_{in}} = 2r_p = \frac{2b_0 V_T}{I_C} = \frac{4b_0 V_T}{I_{bias}} \xrightarrow{b_0=80} \frac{8\,M\Omega}{I_{bias}[mA]} \quad (1)$$

where the parameters of the transistors are defined in [2]. In addition to this, using the expression of Wilson current mirrors output resistance (2), OTA's output resistance (the parallel combination of NPN and PNP Wilson current mirrors output resistance) results in (3):

$$R_0 \approx b_0 \frac{r_0}{2} = \frac{b_0 \cdot V_A}{I_{abc}} \quad (2)$$

$$R_0 = R_{0NPN} // R_{0PNP} = \frac{8G\Omega}{I_{bias}[mA]} // \frac{3.375G\Omega}{I_{bias}[mA]} \approx \frac{2.4G\Omega}{I_{bias}[mA]} \quad (3)$$

These expressions agree with the information in manufacturer's data sheet curves. The most outstanding characteristic of these impedances is their dependence on external control current. In addition to this, input and output capacitances have values of $C_{IN} \approx C_{OUT} \approx 4.5pF$, nearly independent of external control current.

2.1 Transconductance Frequency Response

Since lateral PNP bipolar transistors appear in the signal path (responsible for the reflection of input differential pair collector currents), it is supposed that their low f_T limit the overall frequency response. Taking into account the block diagram of fig.1, the frequency response of the transconductance, defined as the transfer from the differential input voltage to output short-circuit current, can be shown to be:

$$g_m(s) = \frac{i_{oSC}(s)}{v_{in}(s)} \approx g_{mo}(I_{bias}) H_{m_{PNP}}(s) \frac{\left[1 + H_{m_{NPN}}(s)\right]}{2} = hI_{ABC}\ H(s) \quad (4)$$

In the derivation of (4), the effect of the differential pair has been neglected due to its inherent good high-frequency performance [3]. The response of the Wilson mirror can be obtained from its DC relationship [4] (considering non-zero base currents and neglecting output resistances):

$$\frac{I_{out}}{I_{in}} = \frac{(1+\frac{2}{b_{pnp}})}{(1+\frac{2}{b_{pnp}}+\frac{2}{b^{2}_{pnp}})} \xrightarrow{b_{pnp}\uparrow\uparrow} \approx 1 \qquad (5)$$

Using in (5) the generalized complex model for the transfer of current in the transistors (6.1) shows that its frequency response is characterized by a zero at about $s \approx -w_T / 2$ and a pair of complex poles at $s \approx -w_T / 2(1 \pm j)$, resulting in a characteristic peaking of its transfer function. Therefore, the integrator model $h_{FE}(s) \approx w_T / s$ for this transistor parameter is suited in this band of frequencies, and the resulting expression in (6.2) is simpler.

$$h_{FE}(s) \approx \frac{b_o}{(1+s\,b_o / w_T)} \qquad (6.1)$$

$$H_{m_{pnp}}(s) = \frac{I_{out}(s)}{I_{in}(s)} = \frac{1+\frac{2}{h_{FEpnp}(s)}}{1+\frac{2}{h_{FE_{pnp}}(s)}+\frac{2}{h_{FEpnp}{}^{2}(s)}} = \frac{1+\frac{2}{w_{T_{pnp}}}s}{1+\frac{2}{w_{Tpnp}}s+\frac{2}{w_{T\,pnp}{}^{2}}s^{2}} \qquad (6.2)$$

Finally, substituting the expressions in (6.2) for NPN and lateral PNP Wilson mirrors in expression (4), yields

$$H(s, I_{bias}) = \frac{(1+\frac{2}{w_{T\,pnp}(I_{bias})}s)}{(1+\frac{2}{w_{T\,pnp}(I_{bias})}s+\frac{2}{w^{2}_{T\,pnp}(I_{bias})}s^{2})} \cdot \frac{(1+\frac{s}{w_{T\,npn}(I_{bias})})^{2}}{(1+\frac{2}{w_{T\,npn}(I_{bias})}s+\frac{2}{w^{2}_{T\,npn}(I_{bias})}s^{2})} \qquad (7)$$

Note the dependence of the frequency response on DC bias current and that this transfer is not just the series cascade of both NPN and PNP responses, due to the internal structure of the OTA. It seems to be a good approximation to consider only the effect of the lateral PNP Wilson mirror in the transfer function, since its response is slower than NPN mirror. However, because of the different dependence (NPN, lateral PNP) of transistor f_T on the control current (I_{bias}), shown in (8), further analysis is needed.

$$f_T = \frac{1}{2p(t_F + \frac{C_{je}+C_{jc}}{g_m})} \xrightarrow{g_m = \frac{I_C}{V_T} = \frac{I_{BIAS}}{2V_T}} f_T = \frac{1}{2p(t_F + 2V_T\frac{C_{je}+C_{jc}}{I_{BIAS}})} \qquad (8)$$

Fig.2 depicts a comparison between f_T parameter in NPN and lateral PNP transistors, I_{bias} varying from $0.1m$A to 1mA. This graph reveals that OTA's frequency response can be finally modeled as in (9) for bias currents above $10m$A.

$$g_m(s) = g_{m_o} H(s) \approx g_{m_o} H_{mPNP}(s) = g_{m_o} \frac{(1+\frac{2}{w_{T\,pnp}}s)}{(1+\frac{2}{w_{T\,pnp}}s+\frac{2}{w^{2}_{T\,pnp}}s^{2})} \qquad (9)$$

SPICE simulation results from the overall frequency response are shown in figure 3(a). From this figure, it can be derived that the approximation in (9), which results in a final phase lag of 90º, is acceptable for frequencies below ~50MHz. The phase of this model (two complex poles, one zero) remains flatter than that of the single-pole models, and since it becomes the phase error in OTA-C integrators, the model can be used to extend designs to higher frequencies. Thus, the model enhances the capability to extend the frequency margin of designs taking into account second order dynamics.

2.2 Control/Output frequency response

Considering a constant value of voltage in OTA's differential input, small-signal variations in bias current will cause variations in output current, and this allows us to define a transfer function. This model is needed when simulating circuits such as modulators, electronically tunable filters or oscillators (VCO) where the input bias current is a time-varying variable.

Internal analysis from fig.1 (block diagram) reveals that the current signal from control is mirrored in the input NPN Wilson mirror (response as in (6)) and then divided into the differential pair transistors (thus resulting in a pole appearing at $s \approx w_{TNPN}$), assuming symmetry. After following this path, the current signal flows through the same resting blocks. Therefore, since the initial path is all NPN-formed, the transfer function can also be modeled (in a certain frequency margin, also below 50Mhz) after (9). Fig.3(b) shows a SPICE simulation and verifies the previous result. Finally, note that all expressions are a function of process parameters (β, V_A, w_T) and thus they are liable of being suited to different manufacturing processes.

3. SIMULATION RESULTS

In order to validate the previous analytical models, obtained after some simplifications, they have been included in a simple macromodel developed with this purpose. Existing macromodels do not include an accurate model of frequency-dependent transconductance nor the effects of bias-dependent impedances [1,6]. Thus, this improved macromodel is suitable for accurate frequency predictions.

The proposed improved macromodel is shown in fig.4 This is a Boyle-type [7] macromodel that includes the key device issues required in the simulation of oscillators or filters including OTAs. The input differential pair (modeled with explicit transistors with no frequency parameters) operates, by itself, as a transconductor block, and thus modeling with a simple structure OTA's most important behavior. Namely,

1.-The nonlinear relationship between the difference in collector currents and differential input voltage, expressed in (10).

$$i_{C1} - i_{C2} = I_{BIAS} tanh(\frac{V_{IN}}{2V_T}) \xrightarrow{V_{IN} < 2V_T} \approx \frac{I_{BIAS}}{2V_T} V_{IN} = g_m V_{IN} \qquad (10)$$

This fact results in the modeling of:

a Input voltage nonlinearity.

b Product of signals V_{IN} and I_{BIAS} (large signal operation).

c Transconductance (g_m) dependence on bias current (linear operation) and on temperature (V_T).

2.- Dependence of OTA's input resistance with bias current, as expressed in (1).

Continuing with the macromodel structure, the frequency shaping stage provides the transfer function obtained in (9), using RLC passive unity-gain networks. Output stage includes a bias dependent current source modeling the bias dependent output resistance (3), and output voltage limit.

In this model the assumption of dynamics separated from nonlinearities has been made. From the internal structure, it can be inferred that the device frequency response is mostly due to slow lateral PNP current mirrors while non-linear effects occur in the input differential pair.

Both large-signal and small-signal simulations are carried out in order to compare the performance of the full-transistor model and the proposed improved macromodel.

3.1 AC small-signal analysis

The circuit used for the evaluation of the AC response of the macromodel is a current controlled impedance depicted in fig. 4(b). The input impedance simulations of the two models b, c are also shown. While the inclusion of an accurate frequency response and bias-dependent parameters in the new macromodel (b) leads to a satisfactory agreement with the full device-level model (a) - predicting the instability-, the manufacturer's model (c) fails to simulate properly the AC performance of this example.

3.2 Transient large-signal analysis

Fig.6(a,b) shows the results of the first transient simulation where the OTA performs as a multiplier in a simple open-loop configuration. While the low level (20mV and 1kHz) of the input signal keeps the OTA's input stage working in its linear region, the high-level sinusoidal bias current, combined with the effect of a 20KΩ output load, results in the saturation of output voltage.

In the other large-signal simulation (fig. 6c), a 0.2V input sinusoidal signal drives the input stage into its nonlinear region, and the frequency is high enough (2 Mhz) to manifest OTA's frequency response. This simulation confirms the previous hypothesis that nonlinear effects and dynamics (frequency response) can be assumed to be caused by separated stages (namely differential pair and PNP Wilson mirror) in the real device. The developed macromodel handles satisfactorily the simulation whereas the manufacturers' macromodel does not perform properly since it is single-pole in nature.

5. CONCLUSIONS

The reported OTA's model includes several effects such as transconductance frequency response and bias dependent input and output impedances. It has been demonstrated that transconductance frequency response's dependence on the bias control current can be neglected for DC bias currents greater than $10\,mA$. The frequency response considering bias current as input signal has been shown to be modeled by the same transfer function.

The inclusion of this analytical model in a simple macromodel results in a better agreement in simulation results compared with previous models. Future applications include the use of the proposed analytical model to improve performance and extend the frequency margin of designs, as well as predicting second order effects in circuit design.

ACKNOWLEDGMENT

This work has been partially supported by the *Polytechnic University of Catalonia* (PR-9512). Eduard Alarcón holds an FI Grant from the *Generalitat de Catalunya*.

REFERENCES

[1] A. Rodriguez-Vazquez, B. Linares-Barranco, J.L. Huertas and E. Sanchez-Sinencio, "On the design of voltage-controlled sinusoidal oscillators using OTAs", *IEEE Trans.*, Feb. 1990, CAS-37, No.2, pp 198-210.

[2] R.L. Geiger, P.E. Allen and N.R. Strader, "VLSI design techniques for analog and digital circuits", McGraw-Hill, 1990.

[3] C. Tomazou, F.J. Lidgey and D.G. Haigh, "*Analogue IC design : The current-mode approach*". London: Peter Peregrinus , 1990.

[4] R.A. Duncan, K.M. Chan and A.S. Sedra, "Designs for a wideband current amplifier and a current conveyor" , *IEEE Trans.*, April 1994, CAS-41, No.4, pp 272-280

[5] C.Plett and M.A.Copeland, "A study of tuning for continuous-time filters using macromodels", *IEEE Trans.*, August 1992, CAS-39, No.8, pp 524-531.

[6] B. Pérez-Verdu *et al.*, "Nonlinear time-domain macromodelling of OTA circuits", *ISCAS'89*.

[7] G.R. Boyle, B.M. Cohn, D.O. Pederson and J.E. Solomon, "Macromodelling of integrated circuit operational amplifiers", *IEEE J. Solid-state ciruits*, vol SC-9, Dec 1974.

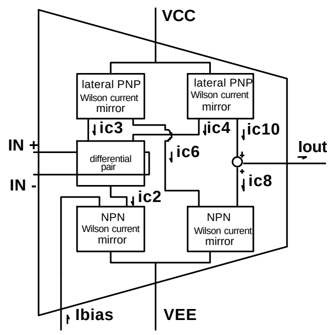

Fig 1. Internal block structure of a commercial OTA

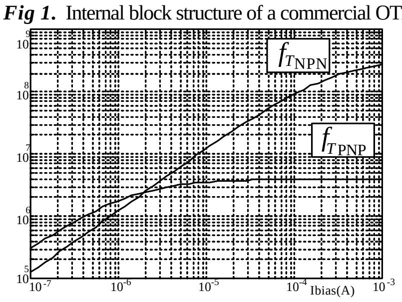

Fig 2. Dependence of transistors' f_T on bias current

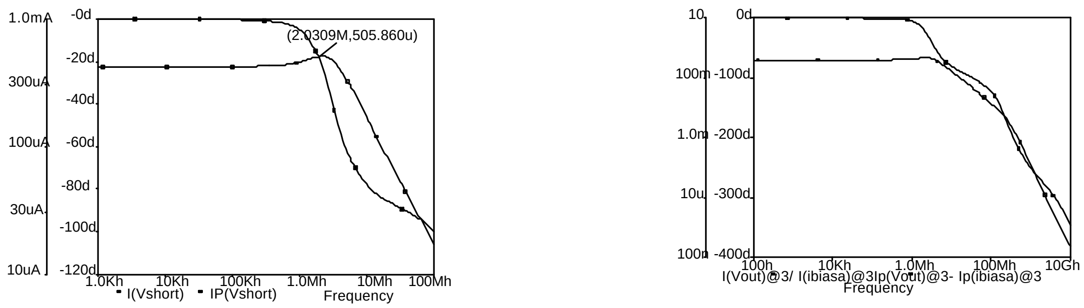

Fig 3. OTA's frequency response. (a) $I_{SC}(s)/V_{IN}(s)$ and (b) $I_{SC}(s)/I_{BIAS}(s)$

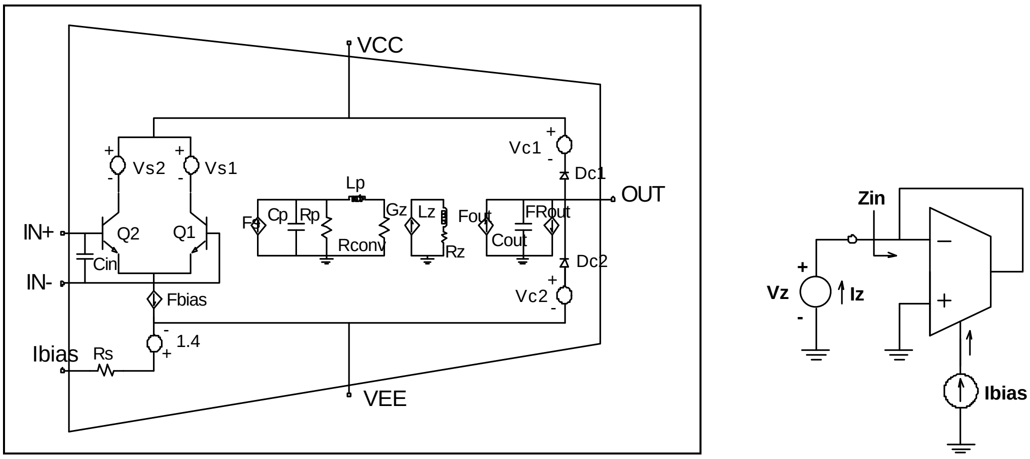

$$Z_{IN}(s) \approx \frac{1}{g_m(s)}$$

Fig 4. (a) Proposed OTA macromodel. (b) circuit for AC simulation

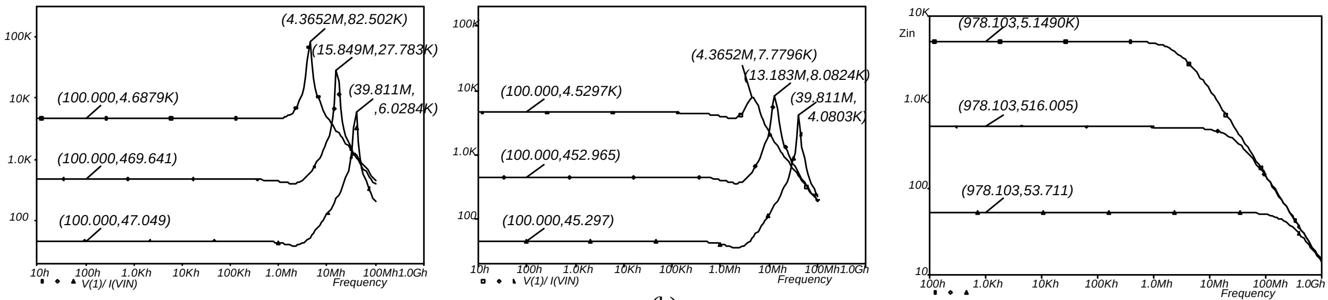

(a) (b) (c)

Fig.5. Z_{in} AC simulations.(a) full transistor. (b) manufacturer's macromodel. (c) new macromodel. (d) simulation circuit.

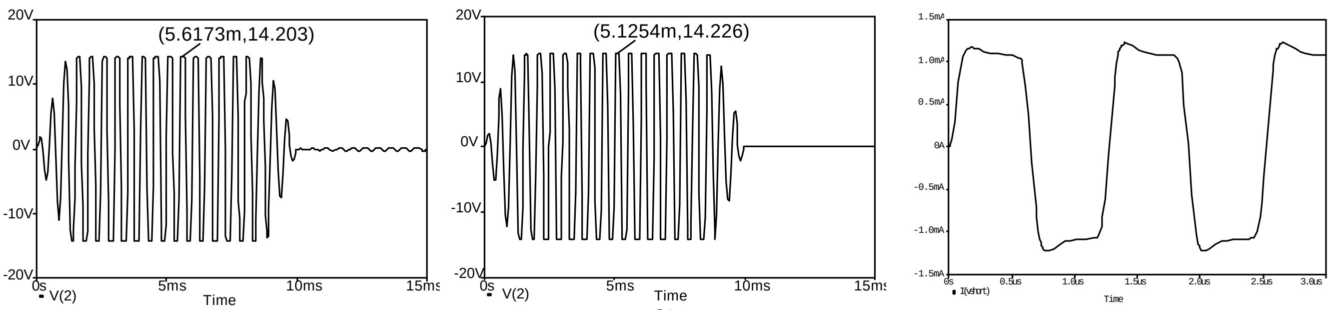

(a) (b) (c)

Fig 6. Simulation output waveforms (a) full model (b) proposed macromodel (c) transistor level transient wich shows separation of linear and nolinear effects